Journal of Sound and Vibration (2001) **240**(5), 937–953
doi:10.1006/jsvi.2000.3267, available online at http://www.idealibrary.com on IDEAL®

VIBRATION ANALYSIS OF ELASTICALLY SUPPORTED TURBOMACHINERY BLADES BY THE MODIFIED DIFFERENTIAL QUADRATURE METHOD

S.-T. Choi and Y.-T. Chou

Institute of Aeronautics and Astronautics, National Cheng Kung University, Tainan, Taiwan 70101, *Republic of China. E-mail: choi@mail.ncku.edu.tw*

(*Received* 23 *May* 2000, *and in final form* 22 *August* 2000)

The modified differential quadrature method (MDQM) is proposed for vibration analysis of elastically supported turbomachinery blades. A pre-twisted blade with varying cross-section is modelled as a Timoshenko beam. The blade is supported by two translational springs and three rotational springs at each end, and has a shroud that is modelled as a mass at the tip of the blade. The equations of motion and the boundary conditions for the coupled flexural and torsional vibration of the blade are obtained by using Hamilton's principle. Numerical results of elastically supported blades with or without a shroud are obtained by the MDQM and are validated by comparing with analytical solutions. Campbell diagrams for a pre-twisted blade with an airfoil cross-section are constructed. The accuracy and efficiency of the present approach have been demonstrated.

1. INTRODUCTION

Turbomachinery is widely used in industry, such as: turboengines, turbogenerators, etc. Failure of turbine blades often occurs as a result of sustained blade vibration at or near their natural frequencies; therefore, knowledge of these frequencies is of fundamental importance. In the past several decades, both analytical methods and experimental techniques have been developed to analyze the vibrational behavior of a rotating blade. Reviews of the various aspects of the blade research can be found in references [1–5]. Carnegie [6, 7] derived the governing equations of motion of a pre-twisted blade of variable cross-section, with the effect of shear deformation and rotary inertia taken into account. Since a closed-form solution for the blade vibration problem is not obtainable, numerical analysis is employed. Fu [8] transformed the Carnegie formulation into a set of recurrence formula and obtained natural frequencies of blades with various end conditions. Maurizi *et al.* [9] considered a uniform Timoshenko beam with ends elastically restrained against rotation and translation and compared the results with that of the Bernoulli–Euler beam. Rossi and Laura [10] studied the transverse vibration of a non-uniform thickness beam having a fixed-end and carrying a concentrated mass at the other. Qatu and Leissa [11] studied vibrations of a laminated composite twisted cantilever plate. Lim and Liew [12] investigated the vibratory characteristics of pre-twisted composite symmetric laminates with trapezoidal platform based on the Ritz method. Lim [13] studied the vibrational behavior of turbomachinery blades with non-linear twisting curvatures and arbitrary angles of twist which are described by a natural twisting co-ordinate system.

0022-460X/01/100937 + 17 $35.00/0

The differential quadrature method (DQM) is a computationally efficient method for solving linear and non-linear partial differential equations. This approach was first proposed by Bellman and Casti [14]. Bert *et al.* [15–17] applied this method to structural problems involving the fourth order partial differential equations. Sherbourne and Pandey [18] analyzed buckling of beams and composite plates by using the DQM. Gutierrez and Laura [19] using the DQM studied the vibrational behavior of the Timoshenko beams. Shu and Richards [20] solved the two-dimensional incompressible Navier–Stokes equation by using a generalized differential quadrature method. Bert and Malik [21] reviewed the recent development of the DQM in computational mechanics. Malik and Bert [22] developed three-dimensional elasticity solutions for free vibrations of rectangular plates by DQM. Choi *et al.* [23] studied the dynamic behavior of an elastically supported spinning Timoshenko beam.

However, there is a major drawback for DQM when dealing with governing equations of fourth or higher orders for which two or more boundary conditions are specified at each boundary point. Numerical error is induced by using the direct deletion or δ-point method in the original DQM since boundary conditions are not exactly satisfied at the boundary points, especially for natural boundary conditions. Choi and Chou [24] proposed the modified differential quadrature method (MDQM) for analyzing various structural elements. This new approach overcomes some drawbacks of the original DQM and provides more accurate solution.

In this paper, the vibrational characteristics of a turbomachinery blade with general end restraints are studied by using the MDQM. The blade is modelled as a Timoshenko beam. The non-dimensional frequencies of a uniform beam with or without a tip mass are obtained and compared with the exact values. Effects of taper ratio and support stiffnesses on the vibrational behavior of a pre-twisted blade are investigated. Campbell diagrams of a pre-twisted asymmetric blade are constructed.

2. EQUATIONS OF MOTION

Figure 1 shows the configuration of an elastically supported blade having a cross-section as an airfoil and a shroud at the tip. The blade which is attached to a rotating hub is supported by two translational springs and three rotational springs at each end. The shroud is modelled as a mass at the tip of the blade and is assumed to have mass m_s, mass moments of inertia I_{dx} and I_{dy} and polar moment of inertia I_θ. The Timoshenko beam theory is adopted and two lateral displacement fields, u and v, and three angular displacement fields,

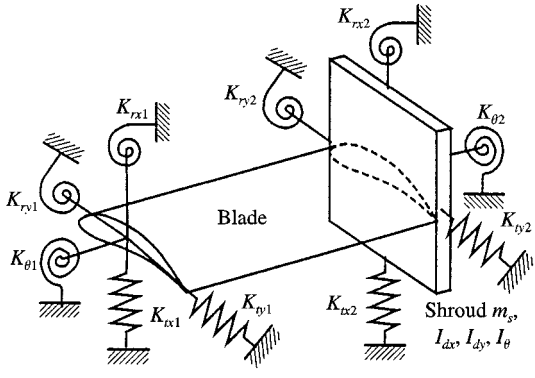

Figure 1. A blade with a shroud and elastic supports.

ϕ_x, ϕ_y and θ on any section of the blade are considered. It is noted that by using a beam model for a blade, the slenderness ratio is limited to a certain value, say, 0·2; otherwise, a plate or shell model should be used.

Figure 2 shows the cross-section of the blade and co-ordinate systems used. X–Y are the principal axes through the centroid of the blade cross-section. x–y are the co-ordinate axes through the centroid and they rotate a twisting angle α with respect to the X–Y co-ordinate. x_1–y_1 are the co-ordinate axes through the center of flexure and are parallel to the x–y axes. ξ–ζ are fixed to the rotating disk and ξ-axis is the spin axis. Both x–y and x_1–y_1 axes are on the cross-section at distance z from the root.

In the present study, the effects of the Coriolis force and the warping of cross-section, as well as the effect of the torsion constant are neglected. Expressions for the kinetic energy and total potential energy of the blade are given in Carnegie [7] and Fu [8]. By using the Hamilton principle and considering free vibration with frequency ω, the equations of motion of the blade are derived as

$$\frac{\mathrm{d}F_x}{\mathrm{d}z} + A\rho\Omega^2 \sin\varphi(u_1 \sin\varphi - v_1 \cos\varphi) + \rho A\omega^2 u_1 = 0, \tag{1}$$

$$\frac{\mathrm{d}F_y}{\mathrm{d}z} + A\rho\Omega^2 \cos\varphi(v_1 \cos\varphi - u_1 \sin\varphi) + \rho A\omega^2 v_1 = 0, \tag{2}$$

$$\frac{\mathrm{d}M_x}{\mathrm{d}z} + \kappa AG(u' - \phi_x) + \rho I_{yy}\omega^2[\phi_x + (r_y\theta)'] = 0, \tag{3}$$

$$\frac{\mathrm{d}M_y}{\mathrm{d}z} + \kappa AG(v' - \phi_y) + \rho I_{xx}\omega^2[\phi_y + (r_x\theta)'] = 0, \tag{4}$$

$$\begin{aligned}\frac{\mathrm{d}T}{\mathrm{d}z} &+ \rho\omega^2 I_{cg}\theta + \rho A r_y\{\omega^2 u_1 + \Omega^2 \sin\varphi(u_1 \sin\varphi - v_1 \cos\varphi)\} \\ &+ \rho A r_x\{\omega^2 v_1 + \Omega^2 \cos\varphi \times (v_1 \cos\varphi - u_1 \sin\varphi)\} + r_y'\{\rho\omega^2 I_{yy}[\phi_x + (r_y\theta)'] \\ &- u_1' \int_z^L \rho A\Omega^2(r + \varsigma)\,\mathrm{d}\varsigma\} + r_x'\{\rho\omega^2 I_{xx}[\phi_y + (r_x\theta)'] - v_1' \int_z^L \rho A\Omega^2(r + \varsigma)\,\mathrm{d}\varsigma\} = 0.\end{aligned} \tag{5}$$

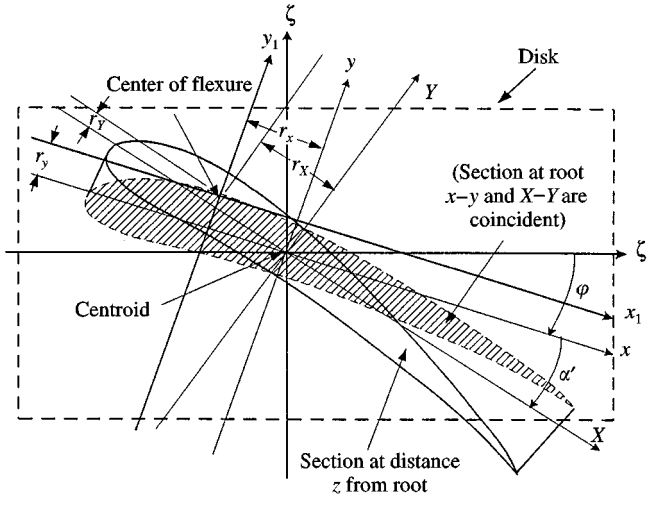

Figure 2. Co-ordinate systems for a turbomachinery blade.

The forcing terms in the above equations are

$$F_x = \kappa AG(u' - \phi_x) + u' \int_z^L A\rho\Omega^2(r + \varsigma)\,\mathrm{d}\varsigma, \tag{6}$$

$$F_y = \kappa AG(v' - \phi_y) + v' \int_z^L A\rho\Omega^2(r + \varsigma)\,\mathrm{d}\varsigma, \tag{7}$$

$$M_x = E(I_{yy}\phi'_x + I_{xy}\phi'_y), \tag{8}$$

$$M_y = E(I_{xx}\phi'_y + I_{xy}\phi'_x), \tag{9}$$

$$T = C\theta' + \rho I_{yy}[\ddot{\phi}_x + (r_y\ddot{\theta})']\, r_y + \rho I_{xx}[\ddot{\phi}_y + (r_x\ddot{\theta})']r_x + (r_y u' + r_x v') \int_z^L A\rho\Omega^2(r + \varsigma)\,\mathrm{d}\varsigma. \tag{10}$$

The boundary conditions are written as

$$z = 0: \quad F_x = K_{tx_1}u, \qquad F_y = K_{ty_1}v, \qquad M_x = K_{rx_1}\phi_x, \qquad M_y = K_{ry_1}\phi_y, \qquad T = K_{\theta_1}\theta, \tag{11a}$$

$$z = L: \quad F_x = -K_{tx_2}u - m_s\omega^2 u, \qquad F_y = -K_{ty_2}v - m_s\omega^2 v,$$
$$M_x = -K_{rx_2}\phi_x - I_{dx}\omega^2\phi_x, \qquad M_y = -K_{ry_2}\phi_y - I_{dy}\omega^2\phi_y,$$
$$T = -K_{\theta_2}\theta - I_\theta\omega^2\theta \tag{11b}$$

3. MODIFIED DIFFERENTIAL QUADRATURE METHOD

The basic concept of the DQM is that the derivative of a function, with respect to a space variable at a given sampling point, is approximated as a weighted linear sum of the functional values at all the sampling points in the domain of that variable. By applying the differential quadrature (DQ) formulation, the partial differential equation is then reduced to a set of algebraic equations for time-independent problems and a set of ordinary differential equations in time for initial/boundary value problems. As for any polynomial approach, the accuracy of the solution by this method increases as the order of the polynomial increases.

For the MDQM, the same procedure of deriving weighting matrices is used as for the original DQM. For a function $u(x)$, the DQ formulation for the first derivative at the ith sampling point is given by

$$\frac{\mathrm{d}}{\mathrm{d}x}u(x_i) \cong \sum_{j=1}^{N} W_{ij}u(x_j), \quad i = 1, 2, \ldots, N, \tag{12}$$

in which N is the number of sampling points, x_i the location of the ith sampling point in the domain, $u(x_i)$ the functional value at this point, and W_{ij} the weighting coefficients of the first-order differentiation.

In order to determine the weighting coefficients W_{ij}, a series of the test functions are taken to be Lagrangian interpolation polynomials [20] as

$$u(x) = \frac{M(x)}{(x - x_i)M_1(x_i)}, \quad i = 1, 2, \ldots, N, \tag{13}$$

where

$$M(x) = \prod_{k=1}^{N} (x - x_k), \qquad M_1(x_i) = \prod_{k=1, k\neq i}^{N} (x_i - x_k), \quad i = 1, 2, \ldots, N.$$

Other types of polynomials could be used as well. However, use of the Lagrangian interpolation polynomial would overcome the numerical ill-condition in calculating the weighting matrix. Introducing equation (13) into equation (12), one derives that

$$W_{ij} = \frac{M_1(x_i)}{(x_i - x_j) M_1(x_j)}, \quad i \neq j \tag{14a}$$

and

$$W_{ii} = -\sum_{j=1, j\neq i}^{N} W_{ij}, \quad i, j = 1, 2, \ldots, N. \tag{14b}$$

For obtaining good accuracy of the analyzed results, it is important to choose appropriate sampling points in the domain. Following Bert and Malik [21], the sampling points are selected as

$$x_i = \frac{L}{2}(1 - \cos[(i-1)\pi/(N-1)]), \quad i = 1, 2, \ldots, N, \tag{15}$$

where L is the length of a beam. Once the sampling points are selected, the weighting matrix can be obtained from equation (14). It is emphasized that the order of the test functions must be greater than the order of highest derivative in the governing equations.

The main difference between the MDQM proposed here and the original DQM is how the boundary conditions are dealt with. In the original DQM, derivatives in the governing equations are directly replaced by weighting matrices and boundary conditions are finally incorporated in the algebraic equations at the boundary points. In the MDQM, governing differential equations, which are written in the first order form, are transformed into algebraic ones by using DQ formulation, and modified relationships are developed for dealing with the boundary conditions so as to overcome the numerical error induced by using the δ-method in the original DQM. A new formulation process is proposed to incorporate the modified relationships and the transformed equations are then combined to obtain the final form of MDQM equations.

3.1. MODIFIED RELATIONSHIP

In MDQM, the functional values of unknown variables are divided into two parts, terms of internal field which are governed by equations of motion, and terms of the given external field which are specified by boundary conditions. As an example, two discretized fields u_i and θ_i, $i = 1, 2, \ldots, N$, are considered for an one-dimensional problem with the boundary conditions $\theta_1 = a_1$ and $\theta_N = a_N$, and θ is the first derivative of u. The relationship by the DQ transformation between θ_i and u_i can be written as

$$\{\theta_i\} = [W_{ij}]\{u_j\}. \tag{16}$$

Considering the boundary conditions $\theta_1 = a_1$ and $\theta_N = a_N$, one obtains the following modified relationship:

$$\{\theta_i^*\} = [B_{ij}^{(\theta)}]\{\theta_j\} + \{C_i^{(\theta)}\}, \tag{17}$$

where

$$\{\theta_i^*\} = \{a_1, \theta_2, \ldots, \theta_{N-1}, a_N\}^{\mathrm{T}},$$

$$[B_{ij}^{(\theta)}] = \begin{bmatrix} 0 & 0 & \cdots & 0 & 0 \\ 0 & 1 & \ldots & 0 & 0 \\ \vdots & \vdots & \ddots & \vdots & \vdots \\ 0 & 0 & \ldots & 1 & 0 \\ 0 & 0 & \ldots & 0 & 0 \end{bmatrix},$$

$$\{C_i^{(\theta)}\} = \{a_1, 0, \ldots, 0, a_N\}^{\mathrm{T}}.$$

$\{\theta_i^*\}$ contains the internal field values of θ and the values at the boundary. $[B_{ij}^{(\theta)}]$ denotes the modified matrix corresponding to the given boundary conditions in θ. $[B_{ij}^{(\theta)}]$ is obtained from an identity matrix by setting to zeros the elements corresponding to the locations of the specified boundary conditions of θ. $\{C_i^{(\theta)}\}$ contains the terms of boundary conditions of θ. If the values of u_i are desired in the previous problem, the DQ formulation of equation (16) can be introduced into the internal field of equation (17) as

$$\{\theta_i^*\} = [B_{ij}^{(\theta)}][W_{jk}]\{u_k\} + \{C_i^{(\theta)}\}. \tag{18}$$

In the case of homogeneous boundary conditions, $\{C_i^{(\theta)}\} = \{0\}$, and the matrix manipulation of equation (18) becomes

$$\{\theta_i^*\} = [B_{ij}^{(\theta)}][W_{jk}]\{u_k\},$$

where

$$[B_{ij}^{(\theta)}][W_{jk}] = \begin{bmatrix} 0 & W_{12} & \cdots & W_{1(N-1)} & 0 \\ 0 & W_{22} & \cdots & W_{2(N-1)} & 0 \\ \vdots & \vdots & \ddots & \vdots & \vdots \\ 0 & W_{N2} & \cdots & W_{N(N-1)} & 0 \end{bmatrix}.$$

This form is the same as that of Bert *et al.* [17].

3.2. NEW FORMULATION PROCESS

In order to use the modified relationships presented in this paper, the governing differential equations of the blade are written in the first order form, as shown in equations (1)–(5). By applying the DQ formulation and introducing the modified relationships, the equations of motion and boundary conditions can be transformed from the differential form to the algebraic form. For example, the boundary conditions of F_x and M_x in equations (11) can be expressed, respectively, as

$$\{F_{x_i}^*\} = [B_{ij}^{(F_x)}]\{F_{x_j}\} + \{C_i^{(F_x)}\}, \tag{19}$$

$$\{M_{x_i}^*\} = [B_{ij}^{(M_x)}]\{M_{x_j}\} + \{C_i^{(M_x)}\}, \tag{20}$$

where

$$\{C_i^{(F_x)}\} = [S_{ij}^t]\{u_j\} + \omega^2[m_{ij}]\{u_j\},$$

$$\{C_i^{(M_x)}\} = [S_{ij}^r]\{\phi_{x_j}\} + \omega^2[J_{ij}]\{\phi_{x_j}\},$$

$$[S^t_{ij}] = \begin{bmatrix} K_{tx^1} & 0 & \dots & 0 & 0 \\ 0 & 0 & \dots & 0 & 0 \\ \vdots & \vdots & \ddots & \vdots & \vdots \\ 0 & 0 & \dots & 0 & 0 \\ 0 & 0 & \dots & 0 & -K_{tx^2} \end{bmatrix}, \qquad [S^r_{ij}] = \begin{bmatrix} K_{rx^1} & 0 & \dots & 0 & 0 \\ 0 & 0 & \dots & 0 & 0 \\ \vdots & \vdots & \ddots & \vdots & \vdots \\ 0 & 0 & \dots & 0 & 0 \\ 0 & 0 & \dots & 0 & -K_{rx^2} \end{bmatrix},$$

$$[m_{ij}] = \begin{bmatrix} 0 & 0 & \dots & 0 & 0 \\ 0 & 0 & \dots & 0 & 0 \\ \vdots & \vdots & \ddots & \vdots & \vdots \\ 0 & 0 & \dots & 0 & 0 \\ 0 & 0 & \dots & 0 & -m_s \end{bmatrix}, \qquad [J_{ij}] = \begin{bmatrix} 0 & 0 & \dots & 0 & 0 \\ 0 & 0 & \dots & 0 & 0 \\ \vdots & \vdots & \ddots & \vdots & \vdots \\ 0 & 0 & \dots & 0 & 0 \\ 0 & 0 & \dots & 0 & -I_{dx} \end{bmatrix}.$$

The governing equations of the blade, equations (1)–(5), and the forcing terms, equations (6)–(10), are to be expressed in the DQ form. By applying the DQ formulation, equation (1) is transformed as,

$$[W_{ik}]\{F^*_{x_j}\} + \rho\Omega^2[A_{ii}]\sin\varphi(\sin\varphi\{u_{1_i}\} - \cos\varphi\{v_{1_i}\}) + \rho\omega^2[A_{ii}]\{u_{1_i}\} = 0, \tag{21}$$

where $[A_{ii}]$ is a diagonal matrix with its ith element equal to the cross-sectional area of the blade at the sampling point z_i. Similarly, equation (6) is transformed into the discrete form and combined with equation (19) as

$$\{F^*_{x_i}\} = [B^{(F_x)}_{ij}](\kappa G[A_{jj}][W_{jk}]\{u_k\} - \kappa G[A_{jj}]\{\phi_{x_j}\} + \rho\Omega^2[R_{jj}][W_{jk}]\{u_k\}) + [S^t_{ij}]\{u_j\} + \omega^2[m_{ij}]\{u_j\}, \tag{22}$$

where $[R_{ii}]$ is a centrifugal force matrix which is expressed as

$$[R_{ii}] = \int_{z_i}^{L} A(z_i)(R + \xi)\,\mathrm{d}\xi.$$

Substituting equation (22) into equation (21), one derives

$$\begin{aligned}(\kappa G[W_{ik}][B^{(F_x)}_{kl}][A_{ll}][W_{lm}] + \rho\Omega^2[W_{ik}][B^{(F_x)}_{kl}][R_{ll}][W_{lm}] + \rho\Omega^2\sin^2\varphi[A_{ij}] \\ + [W_{ij}][S^t_{jm}])\{u_m\} - \rho\Omega^2\sin\varphi\cos\varphi[A_{ij}]\{v_j\} - \kappa G[W_{ik}][B^{(F_x)}_{kl}][A_{lj}]\{\phi_{x_j}\} \\ + \rho\Omega^2([W_{ik}][B^{(F_x)}_{kj}][r'_{y_{jj}}][R_{jj}] + [W_{ik}][B^{(F_x)}_{kj}][R_{ll}][W_{lj}] + \sin^2\varphi[A_{ij}][r_{y_{jj}}] \\ - \sin\varphi\cos\varphi[A_{ij}][r_{x_{jj}}])\{\theta_j\} = \rho\omega^2([A_{ij}] + [W_{ij}][m_{jj}])\{u_j\} + \rho\omega^2[A_{ij}][r_{y_{jj}}]\{\theta_j\}.\end{aligned} \tag{23}$$

Following the same procedure, the rest of the equations of motion and boundary conditions are transformed to the discrete equations and rearranged as follows

$$[K_{ij}]\{w_j\} + \omega^2[M_{ij}]\{w_j\} = 0, \tag{24}$$

where

$$[K_{ij}] = \begin{bmatrix} K_{11} & K_{12} & K_{13} & 0 & K_{15} \\ K_{21} & K_{22} & 0 & K_{24} & K_{25} \\ K_{31} & 0 & K_{33} & K_{34} & 0 \\ 0 & K_{42} & K_{43} & K_{44} & 0 \\ K_{51} & K_{52} & 0 & 0 & K_{55} \end{bmatrix},$$

$$[M_{ij}] = \begin{bmatrix} M_{11} & 0 & 0 & 0 & M_{15} \\ 0 & M_{22} & 0 & 0 & M_{25} \\ 0 & 0 & M_{33} & 0 & M_{35} \\ 0 & 0 & 0 & M_{44} & M_{45} \\ M_{51} & M_{52} & M_{53} & M_{54} & M_{55} \end{bmatrix},$$

$$\{w_j\} = \{u_j \;\; v_j \;\; \phi_{x_j} \;\; \phi_{y_j} \;\; \theta_j\}^{\mathrm{T}}.$$

The elements of $[K_{ij}]$ and $[M_{ij}]$ are presented in Appendix A.

4. RESULTS AND DISCUSSION

The convergence and accuracy of the MDQM are investigated by considering a uniform cantilever Timoshenko beam with a circular cross-section and a slenderness ratio $r/L = 0{\cdot}1$. Numerical results of the first four non-dimensional natural frequencies are obtained by the present approach and listed in Table 1 for different numbers of the sampling points, $N = 7$, 9 and 11. Also shown in Table 1 are the corresponding exact values from Carr [25]. From Table 1, it is observed that the first two natural frequencies converge to the corresponding exact values for $N = 11$, and the third and fourth natural frequencies show their convergence trend. This shows the excellent agreement between the present results and the exact values.

TABLE 1

Non-dimensional frequencies of a uniform cantilever Timoshenko beam by the MDQM and exact solutions $\varpi = \omega(EI/\rho A)^{1/2}/L^2$

	Exact values	MDQM		
Mode	[25]	$N = 7$	$N = 9$	$N = 11$
1	3·324	3·324 (0%)†	3.324 (0%)	3.324 (0%)
2	16·289	16·274 (− 0·09%)	16·289 (0%)	16·289 (0%)
3	36·708	37·079 (1·01%)	36·677 (0·08%)	36·708 (0%)
4	58·279	46·790 (− 19·71%)	57·201 (− 1·85%)	58·278 (0·00%)

† Percent error with respect to exact solution.

For a uniform cantilever beam with circular cross-section and a concentrated mass at the free end, the first five non-dimensional natural frequencies obtained by the MDQM are listed in Table 2 together with the analytical solutions by Rossi *et al.* [10]. Good agreement is again observed from the comparison of these results. This shows the capability of the present approach for dealing with a cantilever beam with a concentrated mass.

The vibration characteristics of a uniform beam with one end fixed and the other end elastically supported and carrying a mass is studied. The slenderness ratio of the beam is taken as $r/L = 0{\cdot}01$ which is small enough such that it behaves like an Euler beam. Non-dimensional fundamental frequencies are obtained by the present approach and are listed in Table 3 for $K_{t2}L^3/EI = 1{\cdot}0$ and different values of m_s/M_b, I_{dx}/M_bL^2 and $K_{rx2}L/EI$. Also listed in Table 3 are results of an Euler beam obtained by Grant [26] using the normal

TABLE 2

Non-dimensional natural frequencies of a cantilever uniform beam with a concentrated mass at the free end (13 *sampling points*)

		Mode									
r/L	$\frac{m_s}{M_b}$	1		2		3		4		5	
		[10]	MDQM	[10]	MDQM	[10]	MDQM	[10]	MDQM	[10]	MDQM
0·01	0·4	2·16	2·1680	17·17	17·1761	52·06	52·0618	106·45	106·4606	180·53	180·3267
	1·0	1·55	1·5574	16·25	16·2499	50·89	50·8944	105·19	105·2003	179·22	179·0412
0·08	0·4	2·14	2·1459	15·92	15·8991	43·74	43·6067	79·81	79·4498	120·69	119·9942
	1·0	1·54	1·5435	15·10	15·0806	42·82	42·5883	78·94	78·5874	119·89	119·2002
0·16	0·4	2·08	2·0840	13·39	13·3347	32·42	32·2145	53·88	53·4596	76·47	75·8153
	1·0	1·50	1·5043	12·76	12·7092	31·76	31·5523	53·32	52·9088	75·79	75·3174

TABLE 3

Non-dimensional fundamental frequency of a uniform beam (*nine sampling points*) $K_{tx2}L^3/EI = 1{\cdot}0$, $r/L = 0{\cdot}01$

		m_s/M_b					
$\frac{K_{rx2}L}{EI}$	$\frac{I_{dx}}{M_bL^2}$	0		1·0		100	
		[26]	MDQM	[26]	MDQM	[26]	MDQM
	0	0·413616	0·413629	0·293137	0·293206	0·099586	0·101806
0·01	1·0	0·293655	0·293653	0·255272	0·254926	0·099543	0·103727
	100	0·099670	0·108500	0·099425	0·099397	0·083880	0·086398
	0	0·931611	0·931613	0·727319	0·727325	0·255535	0·255880
1·0	1·0	0·795710	0·759701	0·681996	0·681983	0·255272	0·255496
	100	0·265809	0·266031	0·265433	0·265650	0·228251	0·229025
	0	0·986917	0·986917	0·808349	0·808347	0·293212	0·293548
100	1·0	0·951724	0·951732	0·794229	0·794233	0·293107	0·293202
	100	0·315401	0·315465	0·315197	0·315381	0·276156	0·276278

mode approach and the Newton–Raphson root finding method. Good agreement is again observed between these two sets of results.

Parametric studies are performed for a Timoshenko beam with a circular cross-section. Effects of the slenderness, taper and mass ratios, and moment of inertia on the fundamental frequency of the beam are investigated.

(1) *Slenderness ratio* (r/L): A uniform Timoshenko beam without an end mass is considered. The non-dimensional fundamental frequency of the beam with different slenderness ratios $r/L = 0{\cdot}01, 0{\cdot}1, 0{\cdot}2$ is obtained by using the MDQM and is shown in Figure 3. It is observed that the fundamental frequency decreases as the slenderness ratio increases since the effect of shear deformation becomes more profound for a higher slenderness ratio.

(2) *Taper ratio* (r_2/r_1): A linearly tapered beam with circular cross-section and slenderness ratio $r_1/L = 0{\cdot}1$ is considered. The non-dimensional fundamental frequency of the beam with different taper ratios $r_2/r_1 = 0{\cdot}5, 1{\cdot}0, 1{\cdot}5$ is obtained by using the MDQM and is shown in Figure 4. It is observed that with r_1/L held fixed, a beam with a higher taper ratio may have a higher or lower fundamental frequency than that of a beam with a smaller taper ratio. The support stiffnesses also play a role in this aspect.

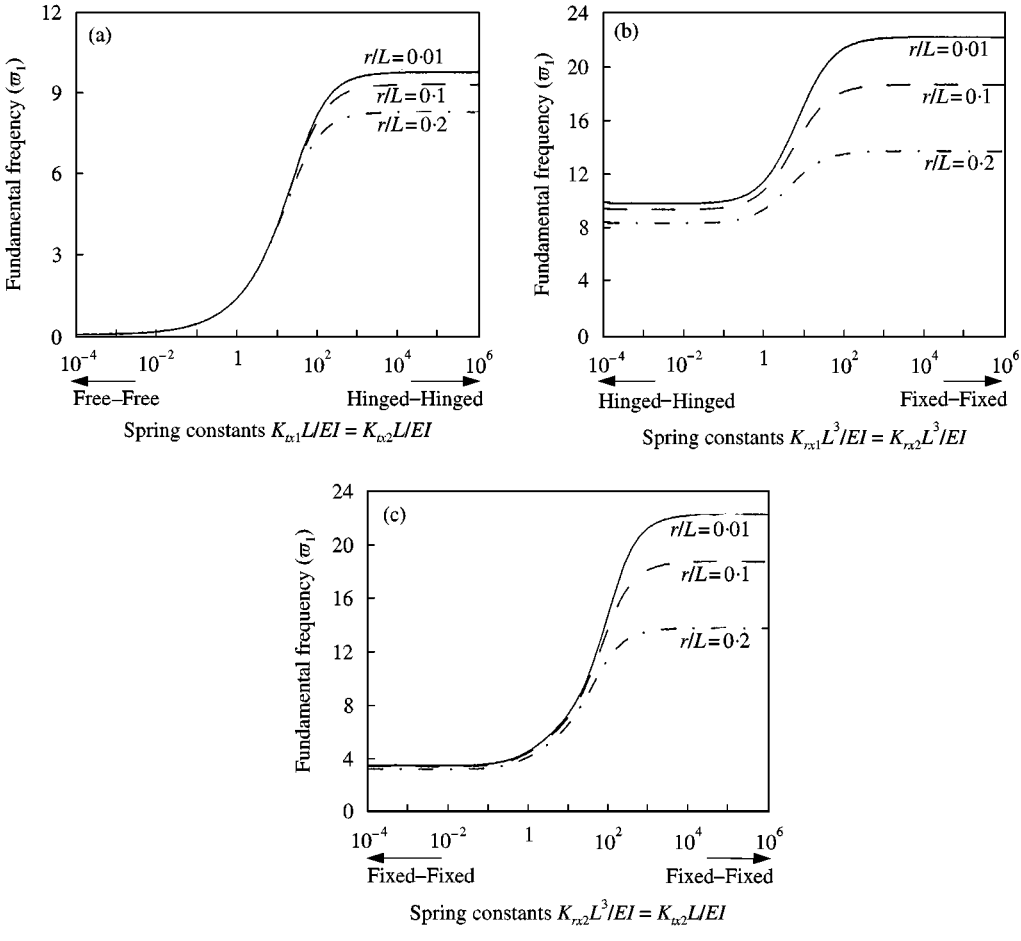

Figure 3. Non-dimensional fundamental frequency of a uniform Timoshenko beam versus the spring constant for various slenderness ratios: (a) $K_{rx1}L^3/EI = K_{rx2}L^3/EI = 0$; (b) $K_{tx1}L/EI = K_{tx2}L/EI = 10^6$; (c) $K_{rx1}L^3/EI = K_{tx1}L/EI = 10^6$.

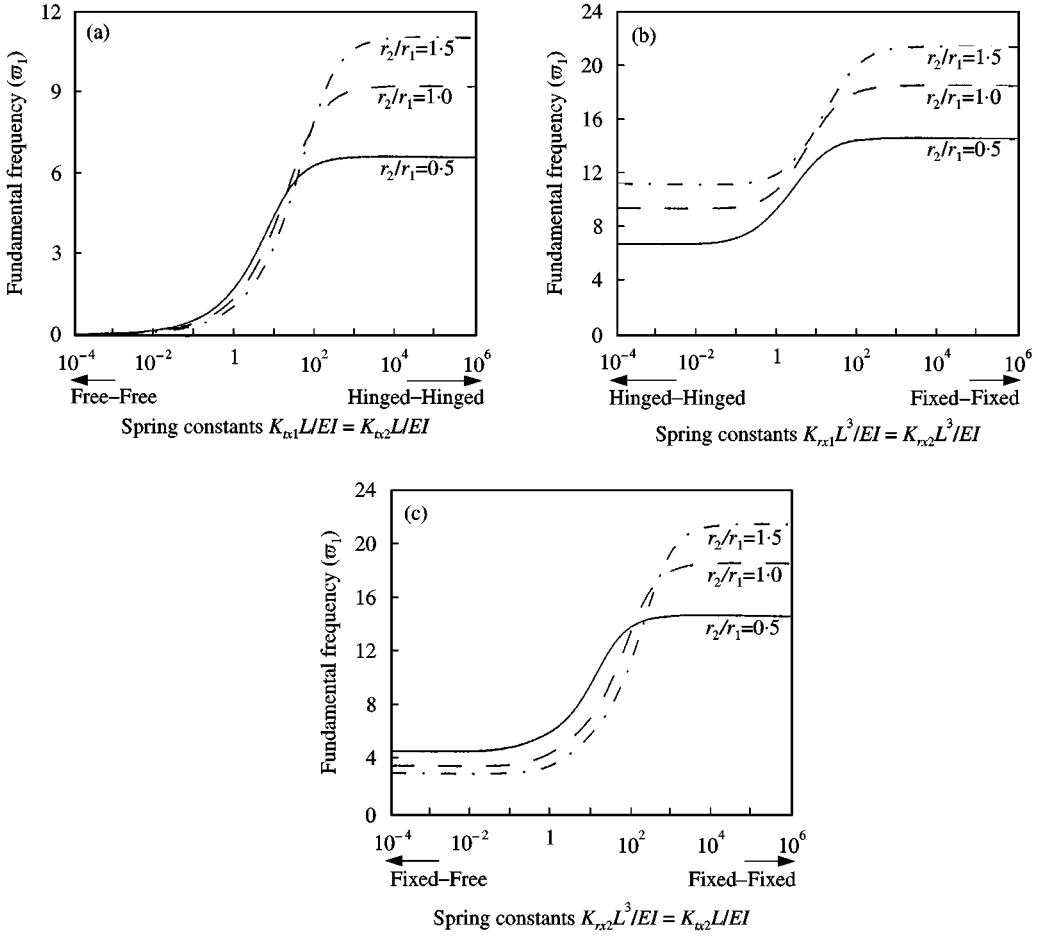

Figure 4. Non-dimensional natural frequency of a Timoshenko beam versus spring constants for various taper ratios ($r_1/L = 0{\cdot}1$): (a) $K_{rx1}L^3/EI = K_{rx2}L^3/EI = 0$; (b) $K_{tx1}L/EI = K_{tx2}L/EI = 10^6$; (c) $K_{rx1}L^3/EI = K_{tx1}L/EI = 10^6$.

(3) *Mass ratio* (m_s/M_b): A uniform beam with a concentrated end mass m_s, and $I_{dx} = I_{dy} = I_\theta = 0$, is studied. The results of non-dimensional fundamental frequency are shown in Figure 5. A higher mass ratio usually results in a lower fundamental frequency. However, the mass ratio does not affect the frequency if the stiffness of the translational spring at the end of the beam, where the mass is attached, is very high such that there is no lateral displacement at that end of the beam.

(4) *Effect of moment of inertia* (I_{dx}/M_bL^2): For a uniform beam having an end mass with mass ratio $m_s/M_b = 1{\cdot}0$ and various moment-of-inertia ratios $I_{dx}/M_bL^2 = 0{\cdot}1$, 1·0, 10, the fundamental frequency is obtained and shown in Figure 6. It is observed that, in general, a higher moment-of-inertia ratio results in a lower fundamental frequency.

The MDQM is applied to determine the natural frequencies of a straight cantilever blade with an airfoil cross-section. The properties of the blade are [27]

$$I_{XX} = 34{\cdot}96\text{e-}12\ \text{m}^4, \quad I_{YY} = 2{\cdot}7928\text{e-}9\ \text{m}^4, \quad L = 0{\cdot}1524\ \text{m}, \quad E = 213{\cdot}9\text{e}9\ \text{Pa},$$

$$\rho = 7{\cdot}8590\text{e}3\ \text{kg/m}^3, \quad A = 58{\cdot}97\text{e-}6\ \text{m}^2, \quad r_X = 0{\cdot}1930\text{e-}3\ \text{m}, \quad r_Y = 1{\cdot}1938\text{e-}3\ \text{m},$$

$$C = 9{\cdot}14\ \text{N m}^2/\text{rad},$$

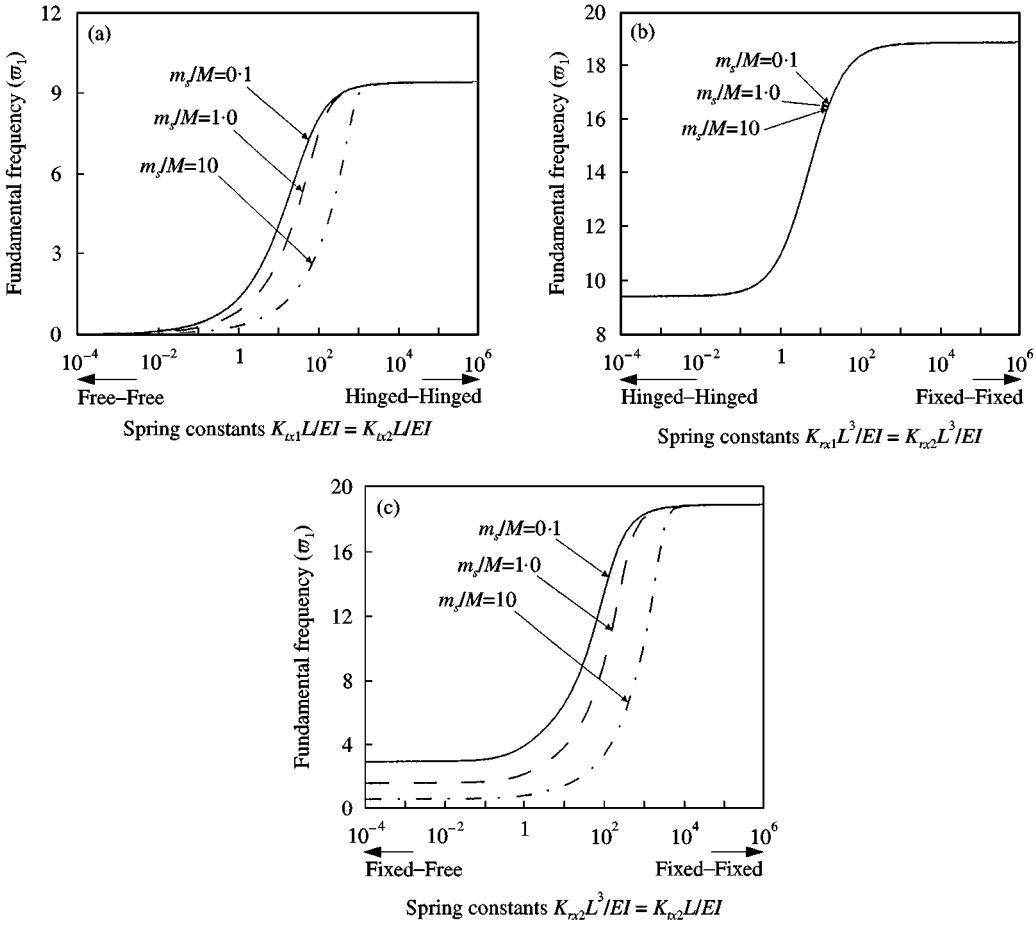

Figure 5. Non-dimensional fundamental frequency of a uniform Timoshenko beam versus spring constants for various mass ratios ($r/L = 0{\cdot}1$): (a) $K_{rx1}L^3/EI = K_{rx2}L^3/EI = 0$; (b) $K_{tx1}L/EI = K_{tx2}L/EI = 10^6$; (c) $K_{rx1}L^3/EI = K_{tx1}L/EI = 10^6$.

The first five natural frequencies of both coupled and uncoupled ($r_X = r_Y = 0$) vibrations obtained by the MDQM are tabulated in Table 4 together with the numerical and experimental results of Rao and Carnegie [27].

As can be observed from Table 4, the coupling effect is not significant in the first three YY bending modes, because the value of r_X is very small. The frequency of the first XX bending dominant coupled mode has reduced considerably from the value of the uncoupled mode, because this mode is affected by r_Y that is much larger than r_X. On the other hand, the frequency of the first torsion dominant mode has increased from the value of the uncoupled mode. Therefore, the effect of asymmetry is such that the natural frequencies of bending vibration decrease and natural frequencies of the torsional vibration increase.

Figure 7 shows the natural frequencies for a blade attached to a hub of radius 0·5 m with a stagger angle $\varphi = 30^\circ$. The geometric properties of the blade are from Sabuncu and Thomas [28]. The natural frequencies of vibration are obtained by the MDQM for the blade with or without a shroud, under different rotating speed Ω of the

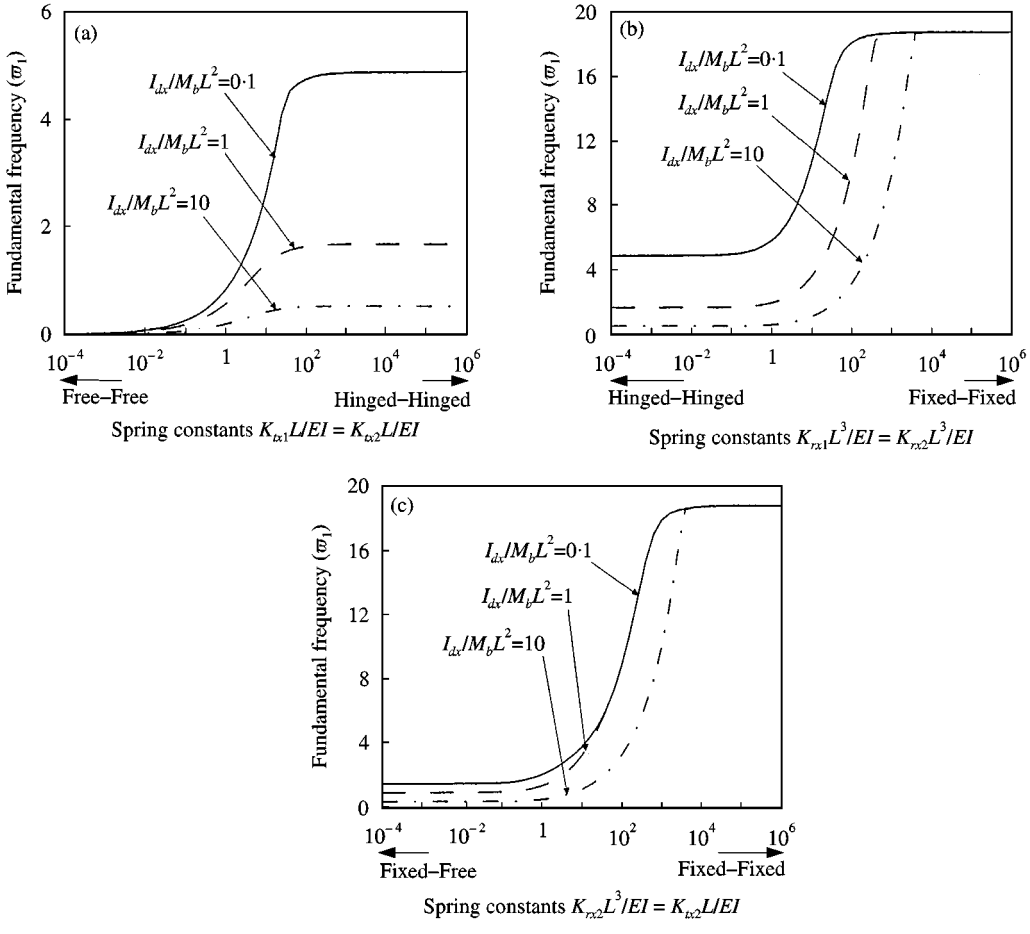

Figure 6. Non-dimensional fundamental frequency of a uniform Timoshenko beam versus spring constants for various moment-of-inertia ratios ($r/L = 0{\cdot}1$, $m_s/M_b = 1{\cdot}0$): (a) $K_{rx1}L^3/EI = K_{rx2}L^3/EI = 0$; (b) $K_{tx1}L/EI = K_{tx2}L/EI = 10^6$; (c) $K_{rx1}L^3/EI = K_{tx1}L/EI = 10^6$.

TABLE 4

Natural frequencies of a cantilever blade with coupled bending-bending-torsion vibration

Mode	Main mode shape	Present result (Hz)		Numerical results (Hz) [27]		Experimental results (Hz) [27]
		Uncoupled	Coupled	Uncoupled	Coupled	
1	*YY* bending	96·76	96·73	96·9	96·9	97·0
2	*YY* bending	605·5	605·3	607·3	607·3	610·0
3	*XX* bending	848·4	810·1	868·4	845·8	790·0
4	Torsion	1045·6	1094·0	1048·23	1074·8	1102·0
5	*YY* bending	1691·4	1690·8	1701·7	1701·6	1693·0

hub. It is expected that when a shroud is added to the blade, the fixed–free condition becomes fixed–hinged or fixed–fixed condition. Consequently, the natural frequencies increase as shown in Figure 7.

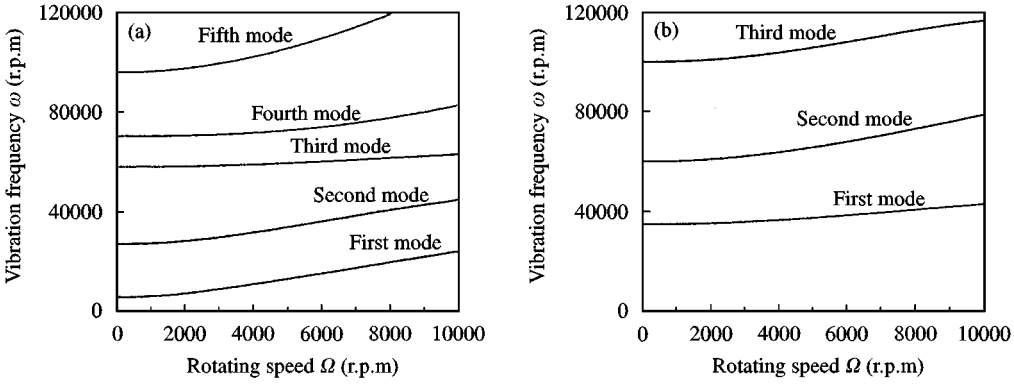

Figure 7. Campbell diagram for an asymmetric blade (a) without or (b) with a shroud.

5. CONCLUSION

The MDQM proposed is applied to dynamic analysis of turbomachinery blades with general end restraints. Contrary to the original DQM, the present approach allows for any combinations of end restraining conditions of blades. Excellent agreements are observed from the comparisons of MDQM results to exact solutions and to those available in the published literature. Effects of the spring coefficients, slenderness, taper and mass ratios on the natural frequency of the blade are examined. Campbell diagrams of an asymmetric blade with or without a shroud are constructed. It has been demonstrated that the MDQM is an accurate and efficient numerical approach for vibration analyses of turbomachinery blades with general end restraints.

REFERENCES

1. A. W. LEISSA 1981 *Applied Mechanics Reviews* **34**, 629–635. Vibrational aspects of rotating turbomachinery blades.
2. A. W. LEISSA and M. S. EWING 1983 *ASME Journal of Engineering for Power* **105**, 383–392. Comparison of beam and shell theories for the vibrations of thin turbomachinery blades.
3. A. W. LEISSA, J. C. MACBAIN and R. E. KIELB 1984 *Journal of Sound and Vibration* **96**, 159–173. Vibration of twisted cantilever plates—summary of previous and current studies.
4. J. S. RAO 1991 *Turbomachine Blade Vibration.* New York: John Wiley & Sons.
5. K. M. LIEW, C. W. LIM and S. KITIPORNCHAI 1997 *Applied Mechanics Reviews* **50**, 431–444. Vibration of shallow shells.
6. W. CARNEGIE 1959 *Proceedings of the Institution of Mechanical Engineers* **173**, 343–374. Vibrations of cantilever blading.
7. W. CARNEGIE 1964 *Journal of Mechanical Engineering Science* **6**, 105–109. Vibrations of pretwisted cantilever blading allowing for rotary inertia and shear deflection.
8. C. C. FU 1974 *International Journal for Numerical Method in Engineering* **8**, 569–588. Computer analysis of a rotating axial-turbomachine blade in coupled bending–bending-torsion vibrations.
9. M. J. MAURIZI, R. E. ROSSI and P. M. BELLES 1990 *Journal of Sound and Vibration* **141**, 359–363. Free vibrations of uniform Timoshenko beams with ends elastically restrained against rotation and translation.
10. R. E. ROSSI, P. A. A. LAURA and R. H. GUTIERREZ 1990 *Journal of Sound and Vibration* **143**, 491–502. A note on transverse vibrations of a Timoshenko beam of non-uniform thickness clamped at one end and carrying a concentrated mass at the other.
11. M. S. QATU and A. W. LEISSA 1991 *International Journal of Mechanical Science* **33**, 927–940. Vibration studies for laminated composite twisted cantilever plates.

12. C. W. LIM and K. M. LIEW 1995 *Acta Mechanica* **111**, 193–208. Vibration of pretwisted cantilever trapezoidal symmetric laminates.
13. C. W. LIM 1999 *Proceedings of Fourth Asia–Pacific Conference on Computational Mechanics, Singapore*, 493–498. Vibration of turbomachinery blades with nonlinear twisting curvature.
14. R. E. BELLMAN and J. CASTI 1971 *Journal of Mathematical Analysis and Applications* **34**, 235–238. Differential quadrature and long-term integration.
15. C. W. BERT, S. K. JANG and A. G. STRIZ 1988 *American Institute of Aeronautics and Astronautics Journal* **26**, 612–618. Two new approximate methods for analyzing free vibration of structural components.
16. S. K. JANG, C. W. BERT and A. G. STRIZ 1989 *International Journal for Numerical Method in Engineering* **28**, 561–577. Application of differential quadrature to static analysis of structural components.
17. C. W. BERT, X. WANG and A. G. STRIZ 1994 *Acta Mechanics* **102**, 11–24. Static and free vibrational beams and plates by differential quadrature method.
18. A. N. SHERBOURNE and M. D. PANDEY 1991 *Computers and Structures* **40**, 903–913. Differential quadrature method in the buckling analysis of beams and composite plates.
19. R. H. GUTIERREZ and P. A. A. LAURA 1994 *Journal of Sound and Vibration* **178**, 269–271. Solution of the Helmholtz equation in a parallelogrammic domain with mixed boundary conditions using the differential quadrature method.
20. C. SHU and B. E. RICHARDS 1992 *International Journal for Numerical Method in Fluids* **15**, 791–798. Application of generalized differential quadrature to solve two-dimensional incompressible Navier–Stokes equations.
21. C. W. BERT and M. MALIK 1996 *Applied Mechanics Review* **49**, 1–28. Differential quadrature method in computational mechanics: a review.
22. M. MALIK and C. W. BERT 1998 *International Journal of Solids and Structures* **35**, 299–318. Three-dimensional elasticity solutions for free vibrations of rectangular plates by the differential quadrature method.
23. S.-T. CHOI, J.-D. WU and Y.-T. CHOU 2000 *American Institute of Aeronautics and Astronautics Journal* **38**, 851–856. Dynamic analysis of a spinning Timoshenko beam by the differential quadrature method.
24. S.-T. CHOI and Y.-T. CHOU 1998 *Proceedings of American Society of Mechanical Engineers International Computer in Engineering Conference, Atlanta, Georgia, U.S.A.* Structural analysis by the differential quadrature method using the modified weighting matrices.
25. J. B. CARR 1970 *Aeronautic Quarterly* **21**, 79–90. The effect of shear flexibility and rotatory inertia on the natural frequencies of uniform beams.
26. D. A. GRANT 1975 *Journal of Applied Mechanics* **42**, 878–880. Vibration frequencies for a uniform beam with one end elastically supported and carrying a mass at the other end.
27. J. S. RAO and W. CARNEGIE 1970 *International Journal of Mechanical Science* **12**, 875–882. Solution of the equations of motion of coupled-bending bending torsion vibrations of turbine blades by the method of Ritz–Galerkin.
28. M. SABUNCU and J. THOMAS 1992 *American Institute of Aeronautics and Astronautics Journal* **30**, 241–250. Vibration characteristics of pretwisted aerofoil cross-section blade packets under rotating conditions.

APPENDIX A

The elements of $[K_{ij}]$ in equation (24) are given as

$$K_{11} = \kappa G W_{ki} B_{ii}^{(F_x)} A_{ii} W_{ij} + \rho\Omega^2 [W_{ki} B_{ii}^{(F_x)} R_{ii} W_{ij} + \sin^2 \varphi A_{jj}] + W_{kj} S_{u_{jj}},$$

$$K_{12} = -\rho\Omega^2 \sin\varphi \cos\varphi \, A_{jj}, \qquad K_{13} = -\kappa G W_{kj} B_{jj}^{(F_x)} A_{jj},$$

$$K_{15} = \rho\Omega^2 [W_{kj} B_{jj}^{(F_x)} r'_{y_{jj}} R_{jj} + W_{ki} B_{ii}^{(F_x)} R_{ii} r_{y_{ii}} W_{ij} + \sin^2 \varphi \, A_{jj} r_{y_{jj}} - \sin\varphi \cos\varphi \, A_{jj} r_{x_{jj}}],$$

$$K_{21} = -\rho\Omega^2 \sin\varphi \cos\varphi \, A_{jj},$$

$$K_{22} = \kappa G W_{ki} B_{ii}^{(F_y)} A_{ii} W_{ij} + \rho\Omega^2 [W_{ki} B_{ii}^{(F_y)} R_{ii} W_{ij} + \cos^2 \varphi \, A_{jj}] + W_{kj} S_{v_{jj}},$$

$$K_{24} = -\kappa G W_{kj} B_{jj}^{(F_y)} A_{jj},$$

$$K_{25} = \rho\Omega^2 [W_{kj} B_{jj}^{(F_y)} r'_{x_{jj}} R_{jj} + W_{ki} B_{ii}^{(F_y)} R_{ii} r_{x_{ii}} W_{ij} + \cos^2\varphi\, A_{jj} r_{x_{jj}} - \sin\varphi\cos\varphi\, A_{jj} r_{y_{jj}}],$$

$$K_{31} = \kappa G A_{ii} W_{ij},$$

$$K_{33} = E W_{ki} B_{ii}^{(M_x)} I_{yy_{ii}} W_{ij} - \kappa G A_{jj} + W_{kj} S_{\phi x_{jj}},$$

$$K_{34} = E W_{ki} B_{ii}^{(M_x)} I_{xy_{ii}} W_{ij}, \qquad K_{42} = \kappa G A_{ii} W_{ij},$$

$$K_{43} = E W_{ki} B_{ii}^{(M_y)} I_{xy_{ii}} W_{ij}, \qquad K_{44} = E W_{ki} B_{ii}^{(M_y)} I_{xx_{ii}} W_{ij} - \kappa G A_{jj} + W_{kj} S_{\phi y_{jj}},$$

$$K_{51} = \rho\Omega^2 [W_{ki} B_{ii}^{(T)} R_{ii} r_{y_{ii}} W_{ij} + \sin^2\varphi\, A_{jj} r_{y_{jj}} - \cos\varphi\sin\varphi\, A_{jj} r_{x_{jj}} - r'_{y_{ii}} R_{ii} W_{ij}],$$

$$K_{52} = \rho\Omega^2 [W_{ki} B_{ii}^{(T)} R_{ii} r_{x_{ii}} W_{ij} + \cos^2\varphi\, A_{jj} r_{x_{jj}} - \cos\varphi\sin\varphi A_{jj} r_{y_{jj}} - r'_{x_{ii}} R_{ii} W_{ij}],$$

$$\begin{aligned} K_{55} = {} & W_{ki} B_{ii}^{(T)} C_{ii} W_{ij} - \rho\Omega^2 R_{ii} [r'^2_{y_{ii}} + r'_{y_{ii}} r_{y_{ii}} W_{ij} + r'^2_{x_{ii}} + r'_{x_{ii}} r_{x_{ii}} W_{ij}] + W_{kj} S_{T_{jj}} \\ & + \rho\Omega^2 [\sin^2\varphi\, A_{jj} r^2_{y_{jj}} - 2\sin\varphi\cos\varphi A_{jj} r_{y_{jj}} r_{x_{jj}} + \cos^2\varphi\, A_{jj} r^2_{x_{jj}}] \\ & + \rho\Omega^2 W_{ki} B_{ii}^{(T)} [r_{y_{ii}} R_{ii} (r'_{y_{ii}} + r_{y_{ii}} W_{ij}) + r_{x_{ii}} R_{ii} (r'_{x_{ii}} + r_{x_{ii}} W_{ij})] \end{aligned}$$

and

$$K_{14} = K_{41} = K_{23} = K_{32} = K_{35} = K_{53} = K_{45} = K_{54} = 0,$$

where W_{ij} denotes the weighting matrix and $B_{ii}^{(\bullet)}$ is the modified matrix; $A_{ii} = A(z_i)$, $I_{xx_{ii}} = I_{xx}(z_i)$, $I_{yy_{ii}} = I_{yy}(z_i)$, $I_{xy_{ii}} = I_{xy}(z_i)$, $r_{x_{ii}} = r_x(z_i)$, $r_{y_{ii}} = r_y(z_i)$, $r'_{x_{ii}} = r'_x(z_i)$, $r'_{y_{ii}} = r'_y(z_i)$, and R_{ii} is a diagonal matrix given as

$$R_{ii} = \int_{z_i}^{L} A(z_i)(R + \varsigma)\, \mathrm{d}\varsigma.$$

The elements of $[M_{ij}]$ in equation (24) are given as

$$M_{11} = \rho A_{jj} + W_{kj} M_{u_{jj}}, \qquad M_{15} = \rho A_{jj} r_{y_{jj}},$$

$$M_{22} = \rho A_{jj} + W_{kj} M_{v_{jj}}, \qquad M_{25} = \rho A_{jj} r_{x_{jj}},$$

$$M_{33} = \rho I_{yy_{jj}} + W_{kj} I_{dx_{jj}}, \qquad M_{35} = \rho I_{yy_{jj}} r'_{y_{jj}} + \rho I_{yy_{ii}} r_{y_{ii}} W_{ij},$$

$$M_{44} = \rho I_{xx_{jj}} + W_{kj} I_{dy_{jj}}, \qquad M_{45} = \rho I_{xx_{jj}} r'_{x_{jj}} + \rho I_{xx_{ii}} r_{x_{ii}} W_{ij},$$

$$M_{51} = \rho A_{jj} r_{y_{jj}}, \qquad M_{52} = \rho A_{jj} r_{x_{jj}},$$

$$M_{53} = \rho W_{kj} B_{jj}^{(T)} I_{yy_{jj}} r_{y_{jj}} + \rho I_{yy_{jj}} r'_{y_{jj}}, \qquad M_{54} = \rho W_{kj} B_{jj}^{(T)} I_{xx_{jj}} r_{x_{jj}} + \rho I_{xx_{jj}} r'_{x_{jj}},$$

$$\begin{aligned} M_{55} = {} & \rho W_{ki} B_{ii}^{(T)} [I_{yy_{ii}} r_{y_{ii}} (r'_{y_{ii}} + r_{y_{ii}} W_{ij}) + I_{xx_{ii}} r_{x_{ii}} (r'_{x_{ii}} + r_{x_{ii}} W_{ij})] + \rho I_{cg_{jj}} \\ & + \rho A_{jj} (r^2_{y_{jj}} + r^2_{x_{jj}}) + \rho I_{yy_{ii}} r'_{y_{ii}} [r'_{y_{ii}} + r_{y_{ii}} W_{ij}] + \rho I_{xx_{ii}} r'_{x_{ii}} [r'_{x_{ii}} + r_{x_{ii}} W_{ij}] + W_{kj} I_{p_{jj}}. \end{aligned}$$

Otherwise $M_{ij} = 0$.

APPENDIX B: NOMENCLATURE

A	cross-sectional area of the blade
C	torsional stiffness
E	Young's modulus of the blade material
G	shear modulus of the blade material
I_{cg}	polar mass moment of inertia about center of gravity
I_{dx}, I_{dy}	mass moment of inertia for shroud about x–y axes
I_{XX}, I_{YY}	principal second moments of area of cross-section
I_{xx}, I_{xy}, I_{yy}	second moments of area of cross-section about x–y axes
I_θ	polar moment of inertia for shroud
K_{tx}, K_{ty}	transverse springs in x- and y-axis
K_{rx}, K_{ry}, K_θ	rotational springs in x-, y- and z-axis
L	length of the blade
M_b	total mass of the beam
m_s	mass of shroud
N	no. of sampling points
R	radius of the rotating disk
r	radius of a circular cross-section of the beam
r_1, r_2	radius of root and tip cross-section of a tapered beam respectively
r_X, r_Y	distances between the center of flexure and centroid in X- and Y-axis
r_x, r_y	distances between the center of flexure and centroid in x- and y- axis
u, v	displacements of center of flexure in x and y directions
u_1, v_1	displacements of centroid in x and y directions
z	distance measured from root
α, α'	pre-twisted angles at the tip and at the section of distance z from root
κ	shear correction factor ($=0{\cdot}833$)
θ	torsional angle
ρ	density per unit volume of the blade material
φ	stagger angle
ϕ_x, ϕ_y	shear angles in x and y directions
ω	natural frequency
Ω	rotating speed of the disk